Article

Eco-Friendly Luminescent Hybrid Materials Based on Eu^{III} and Li^{I} Co-Doped Chitosan

Raquel Alves,[a] Leandro P. Ravaro,[b] Agnieszka Pawlicka,[c] Maria Manuela Silva,[a] and Andrea S. S. de Camargo*,[b]*

[a]*Centro de Química, Universidade do Minho, Gualtar, 4710-057 Braga, Portugal*

[b]*Instituto de Física de São Carlos and [c]Instituto de Química de São Carlos, Universidade de São Paulo, 13566-590 São Carlos-SP, Brazil*

Biopolymer-based materials have been of particular interest as alternatives to synthetic polymers due to their low toxicity, biodegradability and biocompatibility. Among them, chitosan is one of the most studied ones and has recently been investigated for the application as solid state polymer electrolytes. Furthermore, it can serve as a host for luminescent species such as rare earth ions, opening up the possibility of combined electro-optical functionality, of particular interest for electroluminescent devices. In this study, we perform a fundamental, initial, investigation of chitosan based luminescent materials doped with Eu^{III} and Li^{I} triflate salts, from the structural, photophysical and conducting points of view. Because the host presents a broad emission band in the blue to green, while Eu^{III} emits in the red, fine-tuning of emission colour and/or generation of white light is proven possible, by proper combination of optimized composition and excitation scheme. Europium lifetimes ($^5D_0$) are in the range 270-350 μs and quantum yields are up to 2%. Although Li^{I} does not interfere with the luminescent properties, it grants ion-conducting properties to the material suggesting that a combination of both properties could be useful in the development of electro-luminescent devices.

Keywords: chitosan, polymer electrolyte, europium, lithium, electroluminescent devices

Introduction

The low toxicity, biodegradability and biocompatibility of chitosan makes it one of the most widely studied polymers from the application point of view. The application areas include waste water treatment, food industry, agriculture, paper and pulp industry, cosmetics, medicine, tissue engineering, bioseparation and biocatalysis.[1-3] From the physicochemical standpoint, chitosan is a water soluble polymer that can be formed into films, hydrogels and scaffolds, under mild acidic conditions. Moreover, the polycationic character confers to chitosan a high affinity for the association and delivery of therapeutic hydrophilic macromolecules such as proteins, hormones and DNA, thus effectively protecting their bioactivity against enzymatic and hydrolytic degradation.[3,4] As chitosan is water soluble, it is possible to mix it with different inorganic salts and produce polymer electrolytes (PEs) for electrochemical devices assembling.[5] PEs are composed of a host macromolecule and a guest salt, and have been widely studied in the field of solid state electrochemistry, because of commercial interest in their application. Polymer electrolytes based on natural polymers have attracted a lot of attention due to their mechanical, optical and electrical properties.[6] The mixed cation approach, which basically involves the use of two guest salts instead of a single one, is attractive and usually results in an improvement of the conductivity of PEs.[7]

Besides the technological aspects, biopolymer based materials call attention for the possibility of developing environmentally friendly (multi)functional materials that can combine, for instance, high ionic conductivity and efficient luminescent properties.[8,9] In this regard, trivalent lanthanide ions are the most studied luminescent species due to their versatile narrow band emissions in a large spectral range (from visible to near-infrared). Application opportunities are found in, but not restricted to, lighting devices, displays, amplifiers and lasers. The long lifetime of the lanthanide ions excited states allows the use of time-resolved spectroscopy to suppress background

*e-mail: nini@quimica.uminho.pt; andreasc@ifsc.usp.br

fluorescence, reaching very low detection limits, which is relevant for biological applications such as biomarkers and cell imaging.[10] Complexes and salts can display high quantum efficiencies in the near-ultraviolet (Ce[III]), visible (Tm[III] in blue; Tb[III] and Er[III] in green; Dy[III] in yellow; Sm[III] in orange; Eu[III] in red) and near-infrared (Nd[III], Er[III], Tm[III] and Yb[III]).

Studies of the family of Eu[III]-doped d-Ut(300)-based di-urethanesils hybrids prepared by the sol-gel process indicate that the materials are promising full colour emitters with quantum yield ranging from 0.7 to 8.1%.[11] Studies of other hybrids co-doped with Eu[III], Tb[III] and Tm[III] have evidenced the chromaticity of the emission, and it was shown that their optical features were strongly influenced by environmental conditions, such as temperature variations, suggesting the application of these materials in sensing.[12] Eu[III]-doped DNA and agar membranes[9] have also been recently investigated, as well as Eu[III]-doped chitosan, which showed interesting spectroscopic properties. Recently, Tsvirko *et al.*[13] have studied absorption, photoluminescence and time resolved decay properties of chitosan films doped with Eu[III] β-diketonate complex. They have observed that these new materials present very efficient luminescence in the visible region with a quantum efficiency of about 47%. Roosen and Binnemans[14] proposed chitosan modified with ethylenediaminetetraacetic acid (EDTA) and diethylenetriaminepentaacetic acid (DTPA) stationary phase for trivalent rare-earth ions separation using dilute nitric acid solution as eluent. Liu *et al.*[15] have studied bio-organic-inorganic hybrids containing silica, chitosan and Eu[III] or Tb[III] ions. They have observed that the Eu[III] ions have the same local coordination in the chitosan core of these core-shell (chitosan-silica) hybrids as in Eu[III] doped chitosan. Additionally, they have also found a small amount of Eu[III] in the silica shell.

Because the host polymer emits broadly in the blue to green spectral region and Eu[III] in the red,[15] the combination offers the possibility of tuning the emission colour and obtaining white light, through control of composition and proper excitation scheme. In this contribution, we extend the investigation to natural-polymer-based membranes, containing Eu[III] and Li[I], which might offer the possibility of increased electrochemical functionality. These new samples can potentially exhibit both the emission properties due to the Eu[III] ions and conductivity due to Li[I] ions, thus they can be potential candidates for electrochemical devices such as displays. To that end, the chitosan-based membranes are characterized not only from their structural and morphological points of view, but also with respect to their ionic conductivity and photophysical properties. The CIE (*Comission Internationale d'Éclairage*) chromaticity coordinates are given for several samples along with the respective quantum yields and excited state lifetime values. To the best of our knowledge, this is the first time such an approach is used for chitosan based materials co-doped with Eu[III] and Li[I] ions.

Experimental

Sample preparation

The electrolytes were prepared according to the following procedure: 0.20 g of chitosan (Sigma-Aldrich; medium molecular weight) was dispersed in 10 mL of 1% acetic acid solution (Sigma-Aldrich) under magnetic stirring over night to complete dissolution. Then, 0.25 g of glycerol (Himedia; 99.5%) and different quantities of europium (Sigma-Aldrich; 98%) and lithium triflate (Sigma-Aldrich; 99.995%) salts were added and the solutions were kept under stirring for a few minutes. Samples have been represented by the notation $ChiEu_nLi_m$, where n is the lanthanide salt mass and m is the lithium salt mass in the electrolytes (Table 1). The viscous solutions were poured on Petri plates and cooled at room temperature to form the electrolyte films. The films were subjected to a final drying procedure during which the temperature was raised from 25 to 60 ºC over a period of two days to form transparent membranes (Figure 1). During this period the oven was periodically evacuated and purged with dry argon. The thickness was determined with a micrometer (Mitutoyo), and varied between 0.070 and 0.175 ± 0.001 mm. After drying, the samples were conditioned in a glovebox under argon atmosphere.

Characterization techniques

The X-ray diffraction measurements were performed at room temperature in a PANalytical X'Pert Pro diffractometer equipped with an X'Celerator detector. The film samples were exposed to monochromated CuK_α radiation with $\lambda = 1.541$ Å over a scattering angle (2θ) range from 3 to 60 º. In these measurements, samples were placed on a Si wafer, in order to minimize diffuse scattering from the substrate.

The surface morphology of the films, prepared at different ratios, was evaluated using scanning electron microscopy (SEM) micrographs, obtained in a LEO 440 instrument. All film samples were pre-coated with a conductive layer of sputtered gold. The micrographs were taken at 10 kV at different magnifications.

Total ionic conductivities of samples were determined using a constant volume support equipped with gold

Table 1. Relevant details of the synthetic procedure of the $ChiEu_nLi_m$ samples

| Sample	$Eu(CF_3SO_3)_3$		$LiCF_3SO_3$		Thickness
	m^a / g	wt.%	m^a / g	wt.%	mm
Chitosan	–	–	–	–	0.145
$ChiEu_{0.05}$	0.05037	20.11	–	–	0.130
$ChiEu_{0.05}Li_{0.09}$	0.05090	14.51	0.09476	27.01	0.069
$ChiEu_{0.05}Li_{0.2}$	0.05605	10.88	0.23535	49.57	0.159
$ChiEu_{0.1}$	0.10270	33.88	–	–	0.109
$ChiEu_{0.1}Li_{0.04}$	0.10197	28.99	0.04412	12.54	0.141
$ChiEu_{0.1}Li_{0.05}$	0.10140	27.75	0.05237	14.33	0.107
$ChiEu_{0.1}Li_{0.1}$	0.10546	25.36	0.10711	25.76	0.077
$ChiEu_{0.25}$	0.25068	55.34	–	–	0.144
$ChiEu_{0.25}Li_{0.05}$	0.25120	50.30	0.04707	9.42	0.170
$ChiEu_{0.3}$	0.30040	59.85	–	–	0.172

aThe balance error was of ±0.00001g.
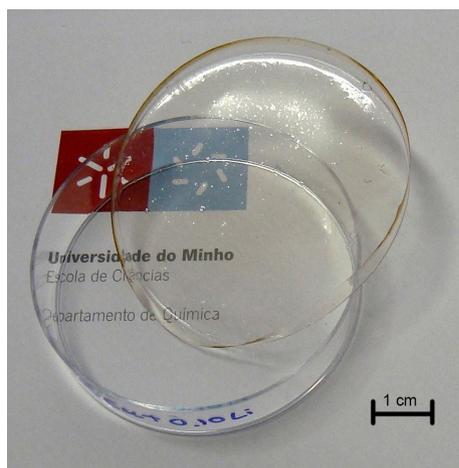
Figure 1. Photograph of a representative $ChiEu_nLi_m$ film. Petri plate diameter was 5.2 cm.

blocking electrodes and located within a Buchi TO 50 oven. The sample temperature was evaluated by means of a type K thermocouple placed close to the electrolyte film and impedance measurements were carried out at frequencies between 65 kHz and 500 mHz using an Autolab PGSTAT-12 (Eco Chemie), over the temperature range 20 to 90 ºC. Measurements of conductivity were effected during heating cycles. The reproducibility of recorded conductivities was confirmed by comparing the results obtained for a sample subjected to two heating-cooling-heating cycles. The excellent reproducibility of the results obtained using this procedure demonstrated the correct operation of the support and the mechanical stability of the samples.

Room temperature emission and excitation spectra of the polymer films, as well as excited state lifetime decays were measured in a Horiba Jobin Yvon spectrofluorimeter model Fluorolog FL3-221 using continuous wave or pulsed (flash) xenon lamps. Quantum yield measurements of Eu-doped and Eu/Li-co-doped samples were carried out in the integrating sphere model Quanta Phi F3029, from Horiba Jobin Yvon, properly connected to the spectrofluorimeter visible detector by optical fibers. By carefully testing various samples, with different sizes, but from the same batch, quantum yields showed a maximum absolute deviation of 10%, so that the presented values are an average.

Results and Discussion

Structural and morphological characterization

Figure 2 depicts the X-ray diffraction (XRD) patterns of film samples of $ChiEu_nLi_m$, i.e., non-doped chitosan and its mixture with either $Eu(CF_3SO_3)_3$ or both $Eu(CF_3SO_3)_3$ and $LiCF_3SO_3$. The diffractograms of all samples, similarly to other ionic conducting membranes based on natural macromolecules, display a broad Gaussian band, centered at ca. 21º that can be assigned to chitosan crystal form type II.[6,16-20] For samples of $ChiEu_{0.1}$ and $ChiEu_{0.1}Li_{0.05}$ the same broad band is observed at 21º, similarly to DNA-Eu^{III} samples.[21] However, as observed in other studies, the doping of polymer matrices with inorganic salts can induce long range disorder in the diffraction patterns.[22] This observation strongly suggests that an increase of the amorphous content was promoted by the presence of salts. As a consequence of the increase of the amorphous content some regions of matrix become more crystaline. Although it seems contradictory, it might be explained as the increased disorder created by the salt among the neighboring chitosan chains forces chain segments, which are not located within the

amorphous domain, to gather in well-defined regions and organize in a more regular manner. Similar behavior was also previously observed for polymer electrolytes based on europium salt and polyethylene oxide (PEO).[23] The polymer electrolytes $ChiEu_{0.1}Li_{0.04}$ and $ChiEu_{0.1}Li_{0.1}$ exhibit Bragg peaks at 21°, similar to $ChiEu_{0.1}Li_{0.0}$, $ChiEu_{0.1}Li_{0.05}$ and non-doped chitosan matrix, and a very sharp lonely peak at 10°. Chitosan powder presents two peaks at $2\theta = 10.9$ and 20.1°.[24,25] The peak at about 10-11° of the $ChiEu_{0.1}Li_{0.04}$ and $ChiEu_{0.1}Li_{0.1}$ is much sharper than the peak of chitosan powder and resemble more the one found in free $LiCF_3SO_3$ or a polymer-salt crystalline complex. Nunes *et al.*[26] also detected a peak at about 10-11° for the system $d-U(2000)_nLiCF_3SO_3$, although this system presents a series of other peaks in salt rich domains. The position of these peaks coincides exactly with the location of the diffraction peaks of the crystalline complex with stoichiometry 3:1 that is formed between PEO and $LiCF_3SO_3$.[27] The peak at 10°, in the present study, can be attributed to the sample or to some impurity. No peak was detected at approximately 29°, which, in the case of the system $U(2000)_nEu(CF_3SO_3)_3$, was ascribed to the diffraction of Eu-rich domains.[28] The obtained results prove that the addition of the guest europium triflate salt to chitosan matrix inhibits the formation of crystalline phases of free $Eu(CF_3SO_3)_3$ or chitosan/salt complexes.

The amorphous nature of the chitosan based electrolyte system provides a clear advantage relative to other semi crystalline systems, since the absence of crystallinity results in improvements in optical, mechanical and electrochemical behavior, especially because ionic movement occurs preferentially in the amorphous phase.[29-31]
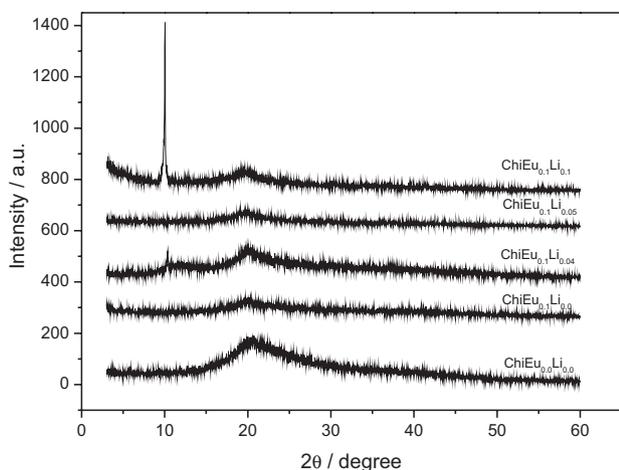

Figure 2. XRD patterns of $ChiEu_nLi_m$ samples.

Scanning electron micrographs illustrating the morphology of chitosan and $Eu(CF_3SO_3)_3$ and $LiCF_3SO_3$ are shown in Figure 3. The good homogeneity without any phase separation and very good surface uniformity at the micrometer scale of samples containing 0.1 g of Eu^{III}-triflate (without Li^I) can be observed in the SEM micrographs in Figure 3a. Similar results were obtained for agar-based films.[32] Other SEM images reproduced in Figure 3 (b, c and d) show that the samples containing mixture of both salts exhibit an irregular texture, and are very similar to the samples of solid polymer electrolyte based on polyethylene glycol (PEG) with high $LiClO_4$ concentration.[22] The micrograph of $ChiEu_{0.1}Li_{0.04}$ (Figure 3b) shows a porous morphology evolving from large to lower pore size. It was verified that this is not a surface effect and it is explained because the degree of porosity is due to the low evaporation temperature of the solvent during the sample preparation. At the same time, the polymer chains show a reduced mobility, which hinder their occupation of the free space left by the evaporated solvent.[33] The images recorded for samples $ChiEu_{0.1}Li_{0.05}$ and $ChiEu_{0.1}Li_{0.1}$ reveal clearer lines that can be either related to undissolved or recrystallized salt, which confirms XRD data.

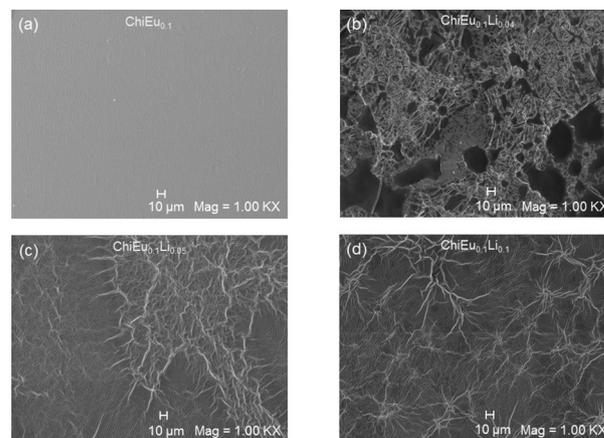**Figure 3.** SEM micrographs of the $ChiEu_{0.1}$ (a) and $ChiEu_{0.1}Li_m$ for m = 0.04 (b); 0.05 (c) and 0.1 (d) samples.

Ionic conductivity of electrolytes

The ionic conductivities of various electrolyte compositions over the temperature range from 20 to 90 °C, and as a function of salt content, are illustrated in Figure 4. These obtained results show a continuous variation in conductivity that is almost linear with respect to 1/T over a range of salt compositions. This plot demonstrates that all the doped samples exhibit a typical behavior for polymer electrolytes where hopping mechanism of ionic charge species is predominant. This behavior is similar to that exhibited by the same matrices doped with different salts[34-36] and contrasts with that of semi-crystalline materials based on commercial polyethylene oxide (PEO) host matrices.[37] The ionic conductivity (σ_i) values were calculated for each heating cycle using the relation of $\sigma_i = d/R_bA$, where

R_b is the bulk resistance, d is the thickness and A is the area of the sample. As shown in Figure 4 (fittings) the ionic conductivity temperature dependence follows the Arrhenius equation of $\sigma_i = \sigma_0 \exp(-E_a/RT)$, where σ_0 is the pre-exponential factor, E_a is the apparent activation energy for ion transport, R is the gas constant (8.314 J mol^{-1} K^{-1}) and T is the temperature.

Table 2 and Figure 4 show the ionic conductivities (σ_i), and activation energy values (E_a), obtained from the above equations.
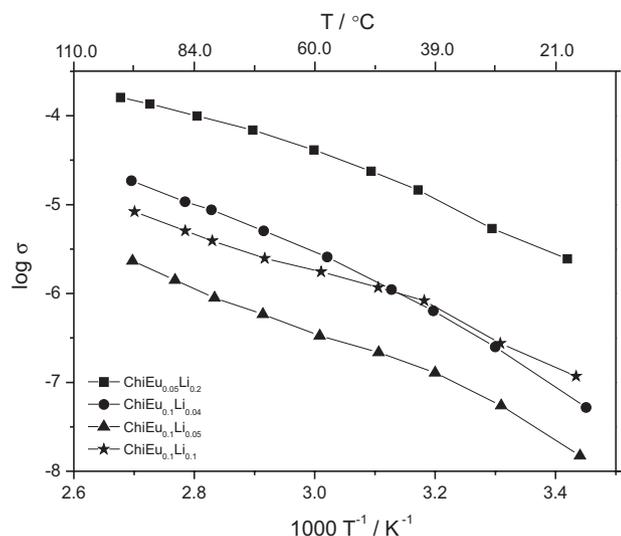

Figure 4. Conductivity plot of the ChiEu$_n$Li$_m$ samples.

Table 2. Ionic conductivity and activation energy of the ChiEu$_n$Li$_m$ samples

Sample	Conductivity / (S cm^{-1})		E_a / (kJ mol^{-1})
	30 ℃	80 ℃	
ChiEu$_{0.3}$	1.58×10^{-8}	3.33×10^{-6}	92.17
ChiEu$_{0.25}$	1.56×10^{-6}	7.57×10^{-5}	64.92
ChiEu$_{0.25}$Li$_{0.05}$	3.14×10^{-8}	4.47×10^{-6}	84.11
ChiEu$_{0.05}$	1.74×10^{-7}	3.45×10^{-6}	57.18
ChiEu$_{0.05}$Li$_{0.09}$	6.66×10^{-8}	1.04×10^{-6}	46.56
ChiEu$_{0.05}$Li$_{0.2}$	5.38×10^{-6}	8.77×10^{-5}	46.93
ChiEu$_{0.1}$	1.57×10^{-7}	1.73×10^{-5}	74.38
ChiEu$_{0.1}$Li$_{0.04}$	1.79×10^{-7}	8.48×10^{-6}	63.30
ChiEu$_{0.1}$Li$_{0.05}$	4.42×10^{-8}	9.07×10^{-7}	52.81
ChiEu$_{0.1}$Li$_{0.1}$	2.32×10^{-7}	3.89×10^{-6}	46.20

Over the whole range of studied temperatures, the sample with the highest ionic conductivity is the ChiEu$_{0.05}$Li$_{0.2}$ with values of 5.38×10^{-6} and 8.77×10^{-5} S cm^{-1}, at 30 and 80 ℃, respectively. These values are higher than those obtained for analogous polymer electrolytes incorporating europium salt[30] and very similar to those doped with lithium salts.[38] Besides temperature, ionic conductivity also depends strongly on the guest salt, both in type and concentration. Usually, increasing guest salt concentration results in an ionic conductivity increase, which is not at all observed in the present study. A high amount of Eu(CF$_3$SO$_3$)$_3$ can play opposite effects. Although the number of charge carriers increases with the increase of salt amount, a high concentration of salt leads to the decrease of free volume, as well as available coordination sites. Additionally, the influence of ion pairing should also be taken into account. The fitted E_a values of all the SPEs are depicted in Table 2, where one can observe that most of E_a values decrease with the increase of ionic conductivity. This behavior was normally expected, since the lower the energy barrier, the easier the ionic movement. This is probably due to the above given reason.

Photophysical properties

Figure 5 presents the photoluminescence emission spectra of the representative sample ChiEu$_{0.3}$ measured with excitation at different wavelengths. Besides the typical bands of Eu^{III} corresponding to transitions from the excited state $^5D_0$ to lower lying ^7F_J states, there is superimposed broad band whose energy in the blue-green spectral region is highly dependent on the chosen excitation wavelength. Similar broad bands have been observed for other bio-polymer hybrid electrolytes and their nature is attributed to the electron-hole recombination in the polymer host.[9,39] At 360 and 394 nm there is concomitant excitation of the Eu^{III} ion and the host, however, at 325 nm (30769 cm^{-1}) only the host is excited (Eu^{III} does not have an energy level corresponding to this wavelength). Therefore, the fact that Eu^{III} emission is observed gives strong evidence of energy transfer from the host to the ion. This assumption is corroborated by examining the excitation spectrum in Figure 6, which was recorded by monitoring the europium emission at 616 nm. In this spectrum, not only the broad polymer band appears, suggesting once again the host → ion energy transfer, but one can also see why excitation at 394 nm is preferable in Eu^{III}-doped systems to achieve higher emission intensities as seen in Figure 5. Furthermore, in the spectra recorded with excitation at 325 and 360 nm, a small structure around 390 nm is observed and it corresponds to self-absorption by the ion. This peak has also been observed in Eu^{III}-based di-ureasil samples.[40] The fact that the $^5D_0 \rightarrow {}^7F_0$ transition band displays only one, well-defined peak, gives strong evidence that the Eu^{III} ion occupies a sole site of symmetry in the SPE samples. Moreover, the considerable intensity (as judged by naked eye) of the hypersensitive transition $^5D_0 \rightarrow {}^7F_2$ with respect to the purely magnetic dipole transition $^5D_0 \rightarrow {}^7F_1$ indicates that such site is of low symmetry, with no inversion center.
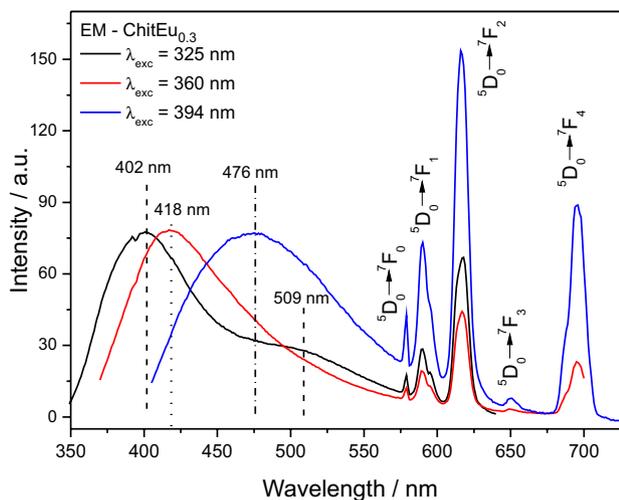
Figure 5. Emission spectra of the sample ChiEu$_{0.3}$ with excitation at different wavelengths. The characteristic transitions of Eu^{III} are indicated nearby the respective bands.
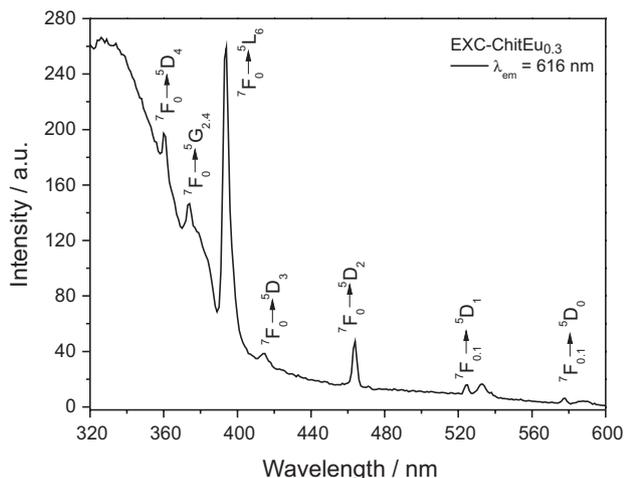

Figure 6. Excitation spectrum of the sample ChiEu$_{0.3}$ measured by monitoring the emission at 616 nm. The characteristic transitions of Eu^{III} are indicated by the respective bands.

The fact that the intense polymer emission accompanies that of Eu^{III}, even when excitation is done at 394 nm, suggests the combination of these bands to generate tunable visible (or white) light.

In Figure 7, a comparison of emission intensities and lineshapes is made for samples co-doped with Li^{I}. It comes out as no surprise that no changes of relative intensities and lineshapes of Eu^{III} bands, as a function of lithium concentration is observed. Still, a new functionality (PEs) is added and could potentially be combined with Eu^{III}-emission in a multifunctional material.

In Figure 8, representative luminescence decay curves measured for the excited state $^5D_0$ by monitoring the emission at 616 nm ($^5D_0 \rightarrow {}^7F_2$) in different ChiEu$_nLi_m$ samples are presented. The sample ChiEu$_{0.3}$ was the only one to display nearly single-exponential decay. However,

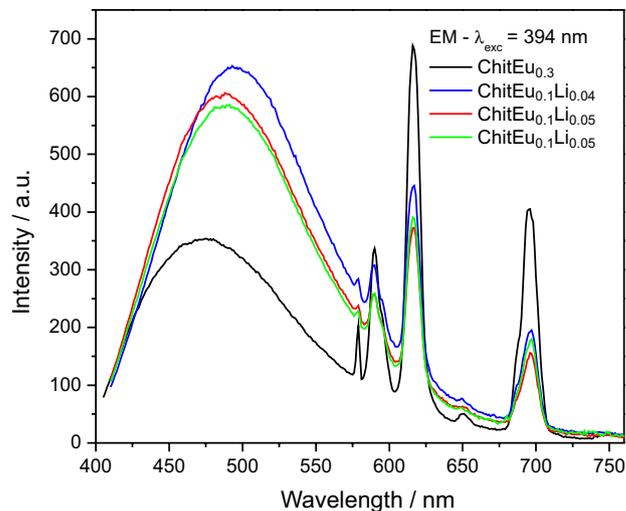**Figure 7.** Comparison of emission spectra of samples doped with different amounts of Eu(CF$_3$SO$_3$)$_3$ and Li(CF$_3$SO$_3$)$_3$. All the spectra were measured with excitation at 394 nm.

for the sake of comparison, averaged lifetime values were determined as the area below the curves corresponding to all samples, and also by assuming the value when intensities drop by a factor 1/e, yielding very similar results. The lifetime values for the samples containing lithium are slightly higher than for the sample, which does not contain this species. The values are in the range of those determined for Eu^{III}-doped agar (194 µs), DNA (528 µs),[9] and for poly(ε-caprolactone)/siloxane biohybrids (225 and 262 µs).[39] In the latter case, the higher value also corresponds to a sample where the Li^{I} concentration is higher indicating that it can be positively interfering by decreasing the amount of hydroxyl ions in the first coordination sphere of the RE ion.

By taking advantage of the concomitant emissions of polymer host and ion, and of the relative intensity variation depending on Eu^{III} concentration and excitation wavelength, the colour tuning[41] can be achieved as indicated in Figure 9.
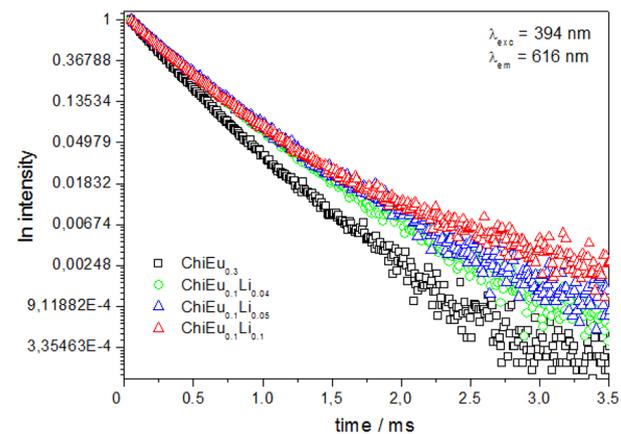

Figure 8. Fluorescence decay curves of ChiEu$_{0.3}$ and ChiEu$_{0.1}$Li$_n$ (n = 0.04, 0.05, 0.1 wt.%) samples determined by single exponential fittings; λ$_{exc}$ = 394 nm, λ$_{em}$= 616 nm.

In Figure 9a, the CIE chromaticity diagram presents the resultant colours for various $ChiEu_mLi_n$ samples, where the $ChiEu_{0.3}$ is closely placed at the crossing of $x = 0.3$ and $y = 0.3$ colour coordinates of the CIE 1931 diagram, upon excitation at 325 nm (Figure 9b). This sample is the closest one to the white in the diagram. The x- and y-chromaticity coordinates are presented in Table 3 for all the samples, together with the quantum yield values φ, measured in an integrating sphere. The maximum φ value around 2.7% is to be expected for Eu^{III} inserted in an environment where hydroxyl groups can act as efficient luminescence quenchers. Still, the values are comparable to other polymer doped hosts[42] and one, possible, way to increase efficiency would be to employ highly coordinated Eu^{III} complexes for which quantum yields can be as high as 85%.[43]
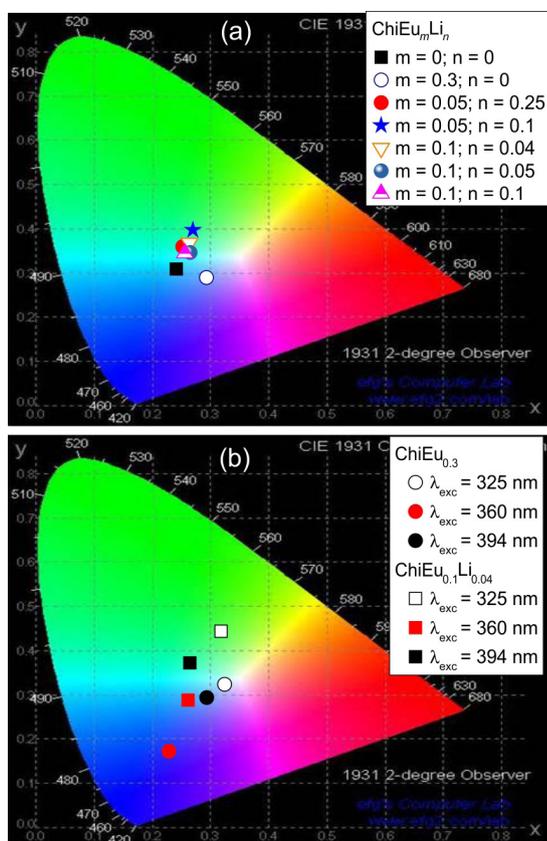
Table 3. Experimental spectroscopic parameters of ChiEuLi samples (excited state $^5D_0$ lifetime τ, absolute quantum yields φ, CIE chromaticity coordinates (x and y))

Sample	τ [$^5D_0$] ± 15% μs	φ ± 10%	CIE x-coordinate	CIE y-coordinate
Chitosan		2.19	0.242	0.317
$ChiEu_{0.3}$	274	1.80 (394 nm)	0.294	0.298
		2.10 (360 nm)	0.229	0.176
		0.57 (325 nm)	0.325	0.328
$ChiEu_{0.05}Li_{0.1}$	341	2.24 (394 nm)	0.271	0.406
$ChiEu_{0.05}Li_{0.25}$	340	2.66 (394 nm)	0.253	0.368
$ChiEu_{0.1}Li_{0.04}$	344	2.40 (394 nm)	0.265	0.377
		0.32 (360 nm)	0.262	0.292
		0.71 (325 nm)	0.319	0.449
$ChiEu_{0.1}Li_{0.05}$	355	2.22 (394 nm)	0.260	0.354
$ChiEu_{0.1}Li_{0.1}$	351	2.30 (394 nm)	0.257	0.353

Ionic conductivity values in the range 5.38×10^{-6} (30 °C) to 8.77×10^{-5} (80 °C) S cm^{-1} were measured, which are higher than those of analogous polymer electrolytes singly doped with Eu^{III} salts, and very similar to those doped with lithium salts.

Photophysical investigations indicate that by combining the emissions of the host matrix and the dopant Eu^{III} ion it is possible to tune the final emission colour and ultimately generate white light. Except for a small increase in europium $^5D_0$ lifetime values (270 to ca. 350 μs), the presence of Li^I does not seem to interfere with the emissive properties, but offers the perspective of further developing and exploring these materials for multifunctional applications. The main benefit of this particular host-ions combination lies in the eco-friendly properties of the biodegradable and non-toxic host.

Figure 9. CIE chromaticity diagrams showing the (x,y) colour coordinates of emissions of $ChiEu_mLi_n$ samples. In (a), the dependence on Eu^{3+} and Li^+ relative concentrations, $\lambda_{exc} = 394$ nm; (b) dependence on excitation wavelength for $ChiEu_{0.3}$ sample.

Conclusions

In this work we developed a novel luminescent and ion conducting biohybrid electrolyte doped with $LiCF_3SO_3$ and $Eu(CF_3SO_3)_3$ by means of the solvent casting method. The Gaussian-shaped broad X-ray diffraction band confirms the predominantly amorphous nature of the studied SPEs.

Acknowledgements

References

1. Kumar, M. N. V. R.; *React. Funct. Polym.* **2000**, *46*, 1.

2. Dutta, J.; Dutta, P. K. In *Chitin and Chitosan: Opportunity & Challenges*; Dutta, P. K., ed.; SSM International Publications: Contai, Midnapore, India, 2005, 1-34.

3. Rinaudo, M.; *Polym. Int.* **2008**, *57*, 397.

4. Rinaudo, M.; *Prog. Polym. Sci.* **2006**, *31*, 603.

5. Cremona, M.; Legnani, C.; Vilani, C.; Calil, V. L.; Barud, H. S.; Quirino, W. G.; Achete, C. A.; Ribeiro, S. J. L.; *Thin Solid Films* **2008**, *517*, 1016.

6. Aziz, N. A.; Majid, S. R.; Arof, A. K.; *J. Non-Cryst. Solids* **2012**, *358*, 1581.

7. Latham, R.; Linford, R.; Pynenburg, R.; Schlindwein, W.; *Electrochim. Acta* **1992**, *37*, 1529.

8. Carlos, L. D.; Ferreira, R. A. S.; Bermudez, V. D.; Julian-Lopez, B.; Escribano, P.; *Chem. Soc. Rev.* **2011**, *40*, 536.

9. Leones, R.; Fernandes, M.; Ferreira, R. A. S.; Cesarino, I.; Lima, J. F.; Carlos, L. D.; Bermudez, V. D. Z.; Magon, C. J.; Donoso, J. P.; Silva, M. M.; Pawlicka, A.; *J. Nanosci. Nanotechnol.* **2014**, *14*, 6685.

10. Bünzli, J. C. G.; Piguet, C.; *Chem. Soc. Rev.* **2005**, *34*, 1048.

11. Goncalves, M.; de Zea-Bermudez, V.; Sá-Ferreira, R.; Carlos, L.; Ostrovskii, D.; Rocha, J.; *Chem. Mater.* **2004**, *16*, 2530.

12. Carlos, L. D.; Sá-Ferreira, R.; Rainho, J.; de Zea-Bermudez, V.; *Adv. Funct. Mater.* **2002**, *12*, 819.

13. Tsvirko, M.; Mandowska, E.; Biernacka, M.; Tkaczyk, S.; Mandowski, A.; *J. Lumin.* **2013**, *143*, 128.

14. Roosen, J.; Binnemans, K.; *J. Mater. Chem. A* **2014**, *2*, 1530.

15. Liu, F.; Carlos, L. D.; Ferreira, R. A.; Rocha, J.; Ferro, M. C.; Tourrette, A.; Quignard, F.; Robitzer, M.; *J. Phys. Chem. B* **2009**, *114*, 77.

16. Pawlicka, A.; Sentanin, F.; Firmino, A.; Grote, J. G.; Kajzar, F.; Rau, I.; *Synth. Met.* **2011**, *161*, 2329.

17. Vieira, D. F.; Pawlicka, A.; *Electrochim. Acta* **2010**, *55*, 1489.

18. Yegorova, A. V.; Scripinets, Y. V.; Duerkop, A.; Karasyov, A. A.; Antonovich, V. P.; Wolfbeis, O. S.; *Anal. Chim. Acta* **2007**, *584*, 260.

19. Song, B.; Vandevyver, C. D. B.; Deiters, E.; Chauvin, A. S.; Hemmila, I.; Bunzli, J. C. G.; *Analyst* **2008**, *133*, 1749.

20. Ogawa, K.; Yui, T.; Okuyama, K.; *Inter. J. Biol. Macromol.* **2004**, *34*, 1.

21. Leones, R.; Rodrigues, L. C.; Fernandes, M.; Ferreira, R. A. S.; Cesarino, I.; Pawlicka, A.; Carlos, L. D.; Bermudez, V. Z.; Silva, M. M.; *J. Electroanal. Chem.* **2013**, *708*, 116.

22. Singh, T. J.; Bhat, S. V. B.; *Mater. Sci.* **2003**, *26*, 707.

23. Smith, M. J.; Silva, C. J. R.; *Solid State Ionics* **1992**, *58*, 269.

24. Wan, Y.; Creber, K. A. M.; Peppley, B.; Bui, V. T.; *Macromol. Chem. Phys.* **2003**, *204*, 850.

25. Pawlicka, A.; Danczuk, M.; Wieczorek, W.; Zygadlo-Monikowska, E.; *J. Phys. Chem. A* **2008**, *112*, 8888.

26. Nunes, S.; de Zea-Bermudez, V.; Ostrovskii, D.; Silva, M. M.; Barros, S.; Smith, M. J.; Carlos, L.; Rocha, J.; Morales, E.; *J. Electrochem. Soc.* **2005**, *152*, 429.

27. Bruce, P. G.; Campbell, S. A.; Lightfoot, P.; Mehta, M. A.; *Solid State Ionics* **1995**, *78*, 191.

28. Zea-Bermudez, V. D.; Carlos, L. D.; Duarte, M. C.; Silva, M. M.; Silva, C. J. R.; Smith, M. J.; Assunção, M.; Alcácer, L.; *J. Alloys Compd.* **1998**, *21*, 275.

29. Leones, R.; Sentanin, F.; Rodrigues, L. C.; Ferreira, R. A. S.; Marrucho, I. M.; Esperança, J. M. S. S.; Pawlicka, A.; Carlos, L. D.; Silva, M. M.; *Optical Mat.* **2012**, *36*, 187.

30. Leones, R.; Sentanin, F.; Rodrigues, L. C.; Marrucho, I. M.; Esperança, J. M. S. S.; Pawlicka, A.; Silva, M. M.; *Express Polym. Lett.* **2012**, *6*, 1007.

31. Gray, F. M.; *Solid Polymer Electrolytes: Fundamentals and Technological Applications*, VCH Publishers Inc.: New York, 1991.

32. Raphael, E.; Avellaneda, C. O.; Manzolli, B.; Pawlicka, A.; *Electrochim. Acta* **2010**, *55*, 1455.

33. Wang, X.; Zhang, L.; Sun, D.; An, Q.; Chen, H.; *Desalination* **2009**, *236*, 170.

34. Barbosa, P.; Rodrigues, L.; Silva, M.; Smith, M.; Gonçalves, A.; Fortunato, E.; *J. Mater. Chem.* **2010**, *20*, 723.

35. Correia, S. G.; de Zea Bermudez, V.; Silva, M. M.; Barros, S.; Ferreira, R. S.; Carlos, L.; Smith, M. J.; *Electrochim. Acta* **2002**, *47*, 2551.

36. Silva, M. M.; de Zea Bermudez, V.; Carlos, L. D.; de Almeida, A. P. P.; Smith, M. J.; *J. Mater. Chem.* **1999**, *9*, 1735.

37. Armand, M.; *Faraday Disc. Chem. Soc.* **1989**, *88*, 65.

38. Nunes, S. C.; Bermudez, V. D.; Silva, M. M.; Smith, M. J.; Morales, E.; Carlos, L. D.; Ferreira, R. A. S.; Rocha, J.; *J. Solid State Electrochem.* **2006**, *10*, 203.

39. Fernandes, M.; Nobre, S. S.; Rodrigues, L. C.; Goncalves, A.; Rego, R.; Oliveira, M. C.; Ferreira, R. A. S.; Fortunato, E.; Silva, M. M.; Carlos, L. D.; Bermudez, V. D.; *ACS Appl. Mater. Inter.* **2011**, *3*, 2953.

40. Gonçalves, M. C.; Bermudez, V. D.; Ferreira, R. A. S.; Carlos, L. D.; Ostrovskii, D.; Rocha, J.; *Chem. Mater.* **2004**, *16*, 2530.

41. Carlos, L. D., Messaddeq, Y.; Brito, H. F.; Sá Ferreira, R. A.; de Zea Bermudez, V.; Ribeiro, S. J. L.; *Adv. Mater.* **2000**, *12*, 594.

42. Sá-Ferreira, R.; Carlos, L.; Gonçalves, R.; Ribeiro, S.; de Zea Bermudez, V.; *Chem. Mater.* **2001**, *13*, 2991.

43. Moudam, O.; Rowan, B. C.; Alamiry, M.; Richardson, P.; Richards, B. S.; Jones, A. C.; Robertson, N.; *Chem. Comm.* **2009**, 6649.

Submitted: June 16, 2015

Published online: October 14, 2015